Pulsed power corona discharges for air pollution control

Pulsed Power Corona Discharges for Air Pollution Control

Erwin H. W. M. Smulders, Bert E. J. M. van Heesch, and Sander S. V. B. van Paasen

***Abstract*— Successful introduction of pulsed corona for industrial purposes very much depends on the reliability of high-voltage and pulsed power technology and on the efficiency of energy transfer. In addition, it is of the utmost importance that adequate electromagnetic compatibility (EMC) is achieved between the high-voltage pulse source and the surrounding equipment.**

Pulsed corona is generated in a pilot unit that produces narrow 50 MW pulses at 1000 pps (net average corona power 1.5 kW). The pilot unit can run continuously for use in industrial applications such as cleaning of gases (100 m^3/h) containing NO or volatile organic compounds (VOC's) or fluids (e.g., waste water). Simultaneous removal of NO and ethylene to obtain clean CO_2 from the exhaust of a combustion engine was tested at an industrial site.

Various chemical processes, such as removal of toluene or styrene from an airflow are tested in the laboratory. We developed a model to analyze the conversion of these pollutants. To examine the discharges in the reactor we use current, voltage, and E-field sensors as well as a fast charge-coupled device (CCD) camera. Detailed energy input measurements are compared with CCD movies to investigate the efficiency of different streamer phases.

EMC techniques incorporated in the pilot unit are based on the successful concept of constructing a low transfer impedance between common mode currents induced by pulsed power and differential mode voltages in signal lines and external main lines.

***Index Terms*— Air pollution control, apparent activation energy, butane, charge-coupled device camera, E-field sensors, electromagnetic compatibility, ethylene, high-voltage, industrial applications, NO, pentane, pilot unit, pulsed corona, pulsed power, pulse source, reliability, streamers, styrene, toluene, transfer impedance, trichloroethane, volatile organic compounds, waste water.**

I. Introduction

HIGH power pulsed corona is a promising type of high-voltage discharge that can be well controlled and has many interesting environmental applications. Energy is deposited in a gas or in a liquid in a highly concentrated form by pulsed corona discharges [1]–[3]. Operating over a wide pressure and temperature range [4], pulsed corona generates electrons, free radicals, excited molecules and, ultraviolet (UV) radiation. Direct bond cleavage or interactions through radicals can breakdown various hazardous organic pollutants. Nonhazardous fragments or compounds that can be further treated using conventional techniques are the result. (e.g., H_2O, CO_2, NO_2, and HCl).

Pulsed corona in water leads to the formation of high local electric fields, electrons, OH^* and H^* radicals, and the repetitive formation of shock waves. In gases, the energized electrons produce radicals through dissociative electron attachment or through electron impact dissociation [5].

Advantages of pulsed corona treatment are: simultaneous removal of several pollutants, high destruction efficiency, no demands on temperature and pressure, insensitive to contamination, no damage from high loads, widely applicable, simply installed, compact, little service, small scale, and no additives.

Specific parameters of the high-voltage pulse are dictated to some extend by the reactor processes. In addition, the parameters are governed by the demand of a match between the pulse source and the transient pulsed corona load. Pulsed corona processing needs pulsed power that is generated in an efficient and reliable way. We investigate whether spark gaps as a reliable long lifetime high-voltage power switch are a good candidate for use in continuous high power industrial applications.

With respect to electromagnetic compatibility (EMC), methods have been developed to effectively suppress interference, in a systematic and reproducible manner, by appropriate guidelines and rules for the layout [6], [7]. Sensitive apparatus for chemical analysis should operate reliably close to the pulse source. Computers and networks in close vicinity and in the surrounding building should remain undisturbed.

II. Pulse Source and Corona Reactor

The pulsed corona unit produces 100 kV pulses (10 ns risetime, 200 ns wide) at a maximum rate of 1000 pulses per second. An overall efficiency of 40–70% was obtained for the energy transfer from mains AC power to corona energy. The mean time between failures for the complete apparatus was approximately 100 h; it was limited by the problem of partial discharge growth toward breakdown in the cable of the transmission line transformer. After improvement of this part, failureless operation now passed the 350 h and is planned to reach 2500 h as testing continues.

Fig. 1 gives an overview of the layout and main components of the pulse source. The corona reactor is placed on top of the main EMC casing. For the production of the high-voltage pulse we use three stages: two resonant circuits coupled by a pulse transformer, followed by a transmission line transformer (TLT) as a third stage [8]. Each stage compresses the pulse duration and raises the pulse amplitude.

Manuscript received October 2, 1997; revised September 10, 1998. This work was supported by The Netherlands Technology Foundation (STW), Convex, and Frigem Energiediensten.

The authors are with the High-Voltage and EMC Group and Process Technology Group, Eindhoven University of Technology, 5600 MB Eindhoven, The Netherlands (e-mail: e.j.m.vanheesch@ele.tue.nl).

Publisher Item Identifier S 0093-3813(98)09083-3.

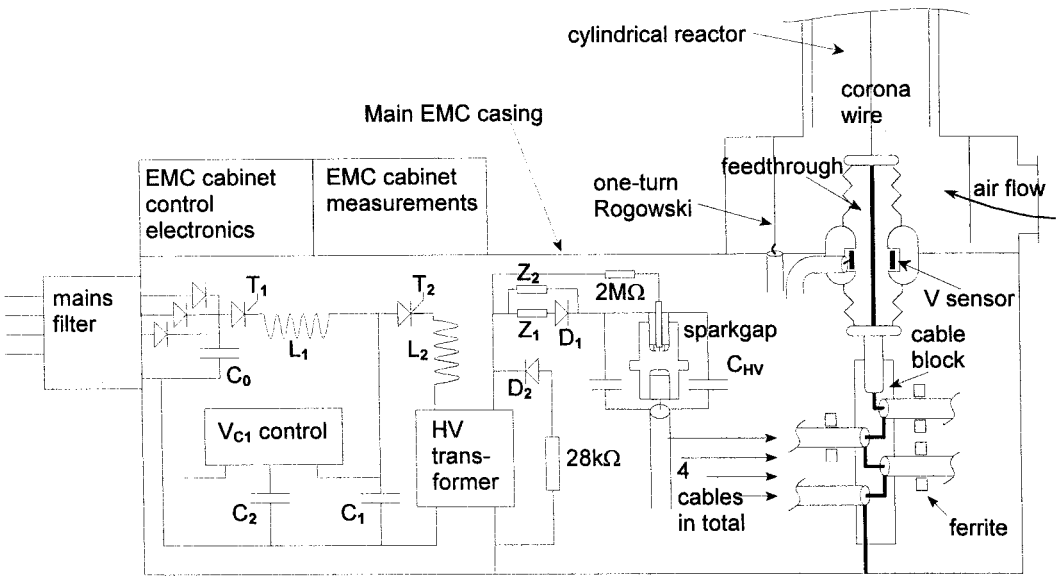

Fig. 1. Schematic overview of the Eindhoven University of Technology (EUT) pilot with high-voltage pulse source. The layout is shown of main components, voltage, and current measuring systems and EMC cabinets. Component values are: $C_0 = 26$ mF, $L_1 = 27$ μH, $C_1 = 12$ μF, $C_2 = 20$ μF, $L_2 = 28$ μH, $C_{\rm HV} = 6$ nF, HV transformer ratio is 10 : 600, and it has two symmetrical coils on a C-core with 0.05 mm core lamination and a core gap of 2 × 0.2 mm. The operation, pulse formation, V_{C1} control, and EMC details as well as the dimensions of the reactor are described in the text.

The first resonant circuit $(C_0, L_1, C_1$ at, respectively, 26 mF, 27 μH, 12 μF) and part of the second resonant circuit $(C_1, L_2 = 28\ \mu$H) are at the low-voltage side (up to 750 V) of the pulse transformer. The pulse transformer (10 : 600) and the high-voltage capacitor $C_{\rm HV}$ (6 nF) to which it is connected complete the second circuit. This capacitor is pulse charged by the resonant circuits in 40 μs to a level of 25–35 kV. The low inductance spark gap (50 nH, coaxial with $C_{\rm HV}$) discharges $C_{\rm HV}$ into the TLT. Diode D_1 (with snubber Z_1, Z_2) holds the voltage at $C_{\rm HV}$. Although the spark gap is free running, an automatic triggering, derived via 2 MΩ from the voltage reversal at the transformer secondary is added to avoid misfiring. The transformer voltage reversal is damped via diode D_2 and the 28 kΩ resistor.

After each high-voltage pulse, part of the energy returns to the low voltage resonant circuits. This surplus of energy depends on the actual breakdown voltage of the spark gap. Depending on the value of this energy, the V_{C1} control system first dumps part of the previously stored energy of buffer capacitor C_2 (20 μF). Next the surplus energy is shared by C_2 and C_1 for partial reuse in the next pulse.

The reliability of the spark gap is excellent, after 10^9 pulses (total transferred charge 200 kC), only minor electrode wear is visible. The gap has to be flushed continuously with air (30 $\rm Nm^3/h$ typically). The spark gap transfers the energy of capacitor $C_{\rm HV}$ to the TLT: four coaxial cables, each 50 Ω and 20 m long (RG214 later replaced by RG218 of 12 m length). We found that four cables is an excellent number with respect to amount of cable, impedance match, and voltage gain. At no load the TLT multiplication ratio is approximately 5.5, resulting in a peak output voltage of 160 kV (10 ns rise time). Loaded by corona the voltage is 100 kV.

Measured voltage and current and calculated power and energy are shown in Figs. 2 and 3. The corona power is the

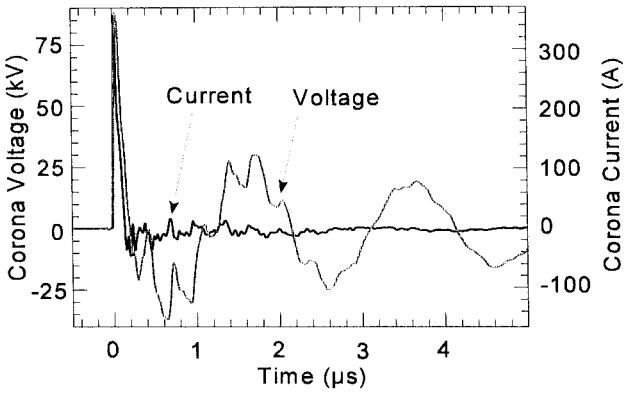

Fig. 2. Typical corona voltage and current pulse. The output high-voltage pulse is measured with a differentiating sensor in the feedthrough; the current pulse is measured with one-turn Rogowski coil at the base of the reactor. Passive integrators for both signals are housed in the EMC cabinet for control electronics.

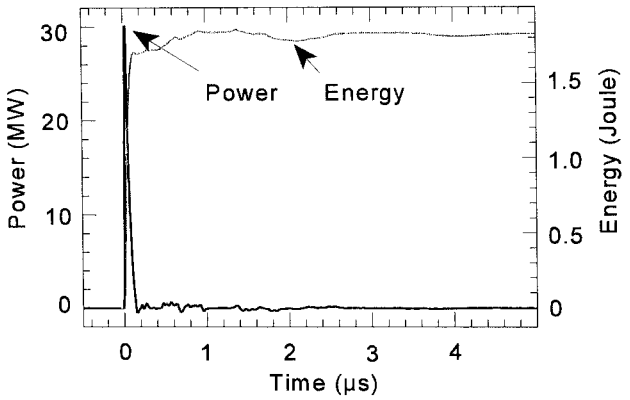

Fig. 3. Power (VI) and energy $(\int VI\ dt)$ of a corona discharge calculated from the measured voltage and current pulses given in Fig. 2.

calculated product (VI) of the measured voltage and current. The energy is the time integral of this product.

The gas to be cleaned flows through the 3.5 m long stainless steel tube reactor, inner diameter 250 mm. The inside wall is smooth or can be fitted with needles. The center electrode is 3 m long, either a wire, diameter 0.25–1.0 mm, or a steel M8 stud. A drawing of the base of the reactor tube and the lower part of the tube (extending unaltered to the end flange) is given in Fig. 1.

III. Measuring Systems

The base of the reactor vessel is a one-turn Rogowski coil (a toroid of rectangular minor cross section) to measure the external (corona) current I_x. The central wire is fed into the reactor via a HV feedthrough, which also contains a capacitive sensor to form a differentiating-integrating (DI) measuring system for the external (corona) voltage V_x [9], [10]. In a DI system it is the strong differentiated signal that is transported via the coaxial cable to the passive *RC* input section of an integrator at the wall of an EMC cabinet. The integrator restores the original waveform but it also acts as an effective EMC filter. Large common mode currents are allowed to flow on the signal cables from sensor to integrator and back via grounding systems. A sufficiently low transfer impedance of these cables leaves the measured signal undisturbed. To avoid interference it is crucial that common mode currents do not enter the EMC cabinet behind the integrator [7]. The bandwidth of the DI systems used is 30 kHz–50 MHz. Passive integrators have been applied. Signal evaluation and corrections for the 50 Ω load of the integrators were made as follows:

$$V_X = k_1 V_{\text{out1}} + \alpha_1 \int k_1 V_{\text{out}}\, dt \tag{1}$$

and

$$I_X = k_2 V_{\text{out2}} + \alpha_2 \int k_2 V_{\text{out2}}\, dt \tag{2}$$

where V_{out1} and V_{out2} are the integrator outputs, k_1 and k_2 are the calibration factors, and α_1 and α_2 are the known correction factors for the integrator droop.

The E field at the cylinder electrode can be measured by means of a grid sensor, mounted flush with the surface of this electrode [11]. Fig. 4 shows the construction of this sensor.

It consists of a measuring electrode (a brass plate with a diameter of 30 mm) behind a grounded stainless steel grid (mesh size 1.4 mm). The distance between the plate and the grid is 2 mm. Charge carriers, which would normally produce a conductive current at the cylinder, are prohibited to enter the grid sensor by a repelling E field between the grounded grid and the plate, which is at a DC bias voltage of 15 V. This bias voltage and the voltage pulse at the central wire have the same polarity. Since the grid is not perfectly shielding, still some 2% of the corona E field is seen by the plate. This transient field produces a displacement current to the plate. The resulting signal is easily distinguished from the DC bias of the sensor. Related techniques to detect the E field are given by other authors [12], [13]. To obtain the total displacement

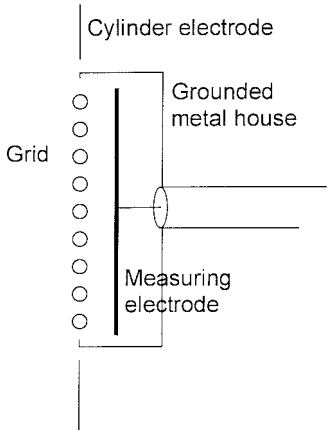

Fig. 4. Construction of the grid sensor that can be used as an E-field sensor if an ion-repelling 15 V DC-bias voltage is applied to the plate. With a forward 900 V DC-bias voltage on the plate it is an ion sensor.

current I_D to the cylinder electrode, the current to the plate of the E-field sensor needs to be multiplied by a factor that accounts for the ratios of surface area and grid penetration. Finally the current must be integrated in the time domain to obtain the displacement charge Q_D, which is proportional to the E field at the cylinder. The bandwidth of this system is 0.5 Hz–50 MHz.

Operating as ion sensor, a forward DC-bias voltage (900 V) on the plate is applied to attract the ions into the grid sensor toward the plate. The resulting conduction current to the plate is a measure for the number of ions arriving at the sensor. The mesh size of the grid is small enough to strongly reduce the corona E field, as is necessary for the ion measurements.

For registrations of the voltage, current, and E-field signals a Nicolet 450 digital oscilloscope, 200 MSa/s, and an HP 54542 A digital oscilloscope, 2 GSa/s were used.

Chemical analysis was done with an HP 5880 gas chromatograph and a flame ionization detector (FID). For propane, butane, pentane, and ethylene a packed column porapak Q was used, for styrene, toluene, and 1,1,1-trichloro-ethane we used a packed SE 54 column. For styrene and toluene temperature programmed runs were made. The NO content of the flue gas of a gas-fueled engine at an industrial site was detected with a chemoluminescence method. All NO measurements in the laboratory were made with a testo 342-2 flue gas analyzer.

In the laboratory, the gas flow to be cleaned was composed by mixing contaminant with an airflow. This mix was fed to the main airflow, produced by pumping environmental air (1.5% H_2O) through the reactor [14]. Main airflow was measured with a testovent 4300 anemometer. Contaminants were fed in through Brooks mass flow controllers. In the case of styrene, toluene, pentane, and 1,1,1 trichloro-ethane, a heated bubbler was used for evaporation. The bubbler was followed by a cool down vessel (20 °C) and the dry airflow into the bubbler was set with a mass flow controller; see Fig. 5. The flow from this system was added to the bulk flow of environmental air through the reactor. In and output concentrations to the reactor were determined from the known input flow and from subsequent measurements with the same instrument while the reactor was in the on or off state.

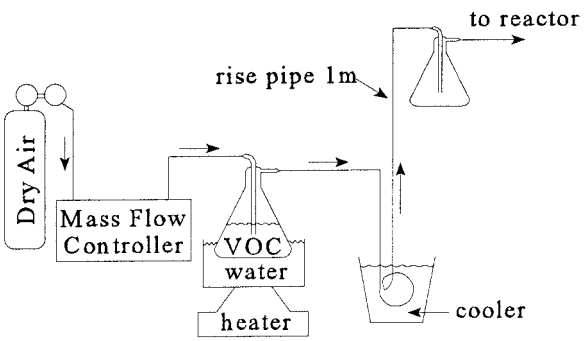

Fig. 5. Installation to produce the VOC vapors to be added to the reactor main flow.

The total corona current, measured externally as I_X, can be represented [1] as a conductive component I_C (passing charge carriers) plus a displacement component (changing E field) I_D. This component, measured separately with the E-field sensor, equals the current I_0 due to the changing external voltage V_X across the vacuum capacitance C_0 between the electrodes, plus the current I_S due to the movement of space charge in the gas

$$I_X = I_C + I_D = I_C + I_0 + I_S \tag{3a}$$

and

$$I_0 = C_0\, dV_X/dt. \tag{3b}$$

A number of CCD images (5 ns gating) are recorded in successive discharges to display the development of the corona discharge. The direction of view of the CCD camera was axial, parallel to the corona wire. CCD images cover the full cross section of the cylindrical reactor. From each recorded image we copy a strip running from wire to wall and combine these strips into one picture, a CCD movie, as shown in Fig. 6.

IV. Discharge Development

Both positive and negative corona show similar behavior. First, many streamers develop from the wire toward the cylinder during the initial streamer phase [1]. The strongly inhomogeneous space charge at the streamer head creates a large E field, which causes an enhanced ionization and further growth of the initial streamers toward the cylinder. Each streamer carries a current of 0.1–1 A. The capacitance between the streamer head and the cylinder acts as a limiting impedance for the current through the initial streamer. The conductive streamer phase starts after the arrival of the initial streamers at the cylinder. The development of the initial streamer into a complete channel between the wire and the cylinder results in a disappearance of the capacitance between the streamer head and the cylinder. This allows a much larger current (1–10 A) to flow through each streamer; many streamers in parallel carry the large current of the pulsed corona discharge.

The curves for the measured charges Q_X (total) and Q_D (displacement only) are equal until the arrival of the initial streamers at the cylinder. After arrival a conductive current at the cylinder causes a separation of the curves Q_X and Q_D. With a negative polarity at the wire, corona also develops at the needles covering the cylinder electrode. The resulting conductive current causes an early separation between the curves Q_X and Q_D.

Based on current and voltage measurements a calculation was made of the energy input during the initial and the conductive streamer phase of a positive polarity discharge. The results are given in Fig. 7. It turns out that after the completion of a pulse, about one third of the corona energy is a result of the initial streamer phase and 2/3 results from the conductive streamer phase. If the indications are correct that the amount of corona energy is the important parameter for chemistry then the conductive streamer phase can add considerably to the conversion process.

V. Reactor Model

An exponential behavior for the VOC's removal by the pulsed corona reactor was found experimentally and was given as [15]

$$X = 1 - \exp(-E/\Delta E). \tag{4}$$

The dimensionless X is the amount removed divided by the amount on input, where both amounts can be consistently expressed either in terms of g/h or as concentration, e.g., mole fraction or parts per million. The parameter E is the applied corona energy per unit volume and it will be shown now that ΔE is an apparent activation energy per unit volume for a mixture of a specific VOC plus air. Within the concentration ranges that we tested this apparent activation energy for the mixture is independent of the VOC's concentration. An analysis based on gas dynamics and reaction kinetics is used to explain the exponential behavior and apparent activation energy. The reactions are activated by use of corona energy in an oxidating environment. Since the concentration of reactants formed in the environmental air by the corona discharge is high compared to the VOC's concentration only first order reactions are considered. As the mechanism for the reaction is not known, an alternative expression for the rate constant k [number of transitions per second] of the reaction will be needed.

With the experimental data we can find Peclet numbers of 10^4–10^5 which means we are dealing with a plug flow reactor. In our tubular plug flow reactor we have Reynolds numbers of 2000–10^4 which means that the flow is turbulent. With this knowledge we can make the following assumptions:

- only energy from the corona discharge is used for decomposition;
- the apparent activation energy is independent of the VOC's concentration (ad hoc, verified by experiment);
- the reactor is an ideal plug flow reactor;
- only first order reactions are considered;
- an alternative expression for the rate constant k is postulated.

A negative free energy change of a reaction means that after the reactions the products are at a lower free energy level. However, if bonds are broken, the reactants must go up an energy hill first, before they will go downhill. The activation of VOC's plus air can be reached by using corona energy [14]. We are concerned about the apparent activation

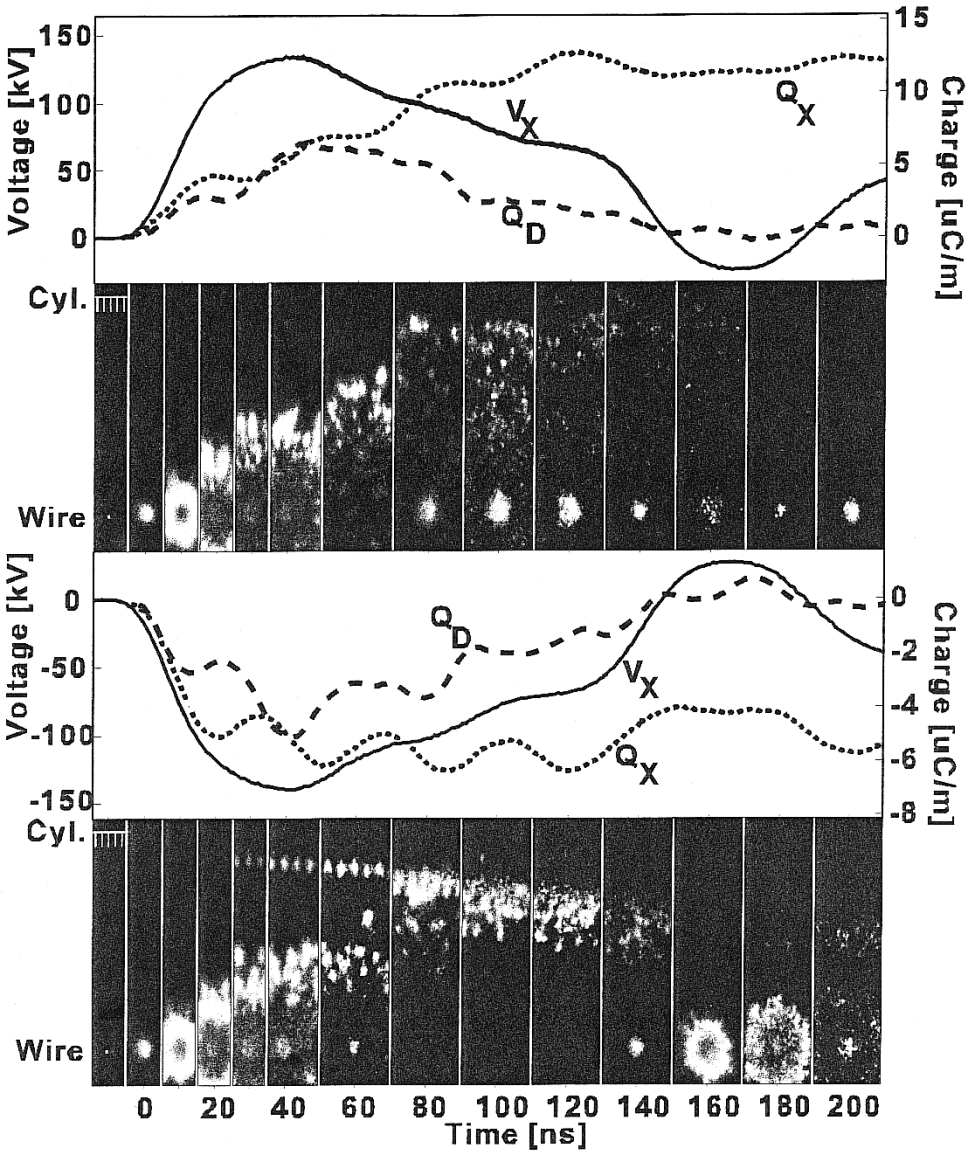

Fig. 6. Discharge development in 560 torr of air and 29 cm diameter cylinder; positive polarity +134 kV (upper half of figure) and negative polarity −140 kV (lower half of figure). CCD movie of discharge development, measured voltage pulse, total, and displacement charge.

energy $\Delta E[J/l]$ needed for the decomposition of VOC's in the mixture. For the rate constant k [number of transitions per second] of the reaction we postulate a simple alternative expression [14]

$$k = \gamma P/\Delta E \tag{5}$$

where P is the corona power per m^3 and γ the used fraction of this power. The apparent activation energy per $m^3, \Delta E$, varies with the concentration of the mixture air plus VOC's

$$\Delta E = \Delta E_0 C_{\mathrm{mix}}/C_{\mathrm{mix0}}. \tag{6}$$

Here C_{mix} is number of moles of mixture per unit volume [mol/m^3] and C_{mix0} and ΔE_0 are the values at standard temperature and pressure (STP) conditions.

The reaction rate R (number of moles converted per second per m^3) of a first order reaction is

$$R = kC. \tag{7}$$

The VOC's concentration is C. The reaction rate is substituted in the continuity equation

$$\partial C/\partial t + u\partial C/\partial z = -R \tag{8}$$

for the flow in the reactor. The flow velocity is u [m/s] in the direction along the axial z coordinate of the cylinder.

To find the stationary solution of (8) we integrate along the length of the reactor and arrive at the desired exponential relation given above in (4).

The exponential relationship is very useful for fitting measured data in many cases. Some removal processes however do not fit the model.

VI. Conversion of VOC's and NO

Simultaneous removal of NO and ethylene to obtain clean CO_2 from the exhaust of a power generating combustion

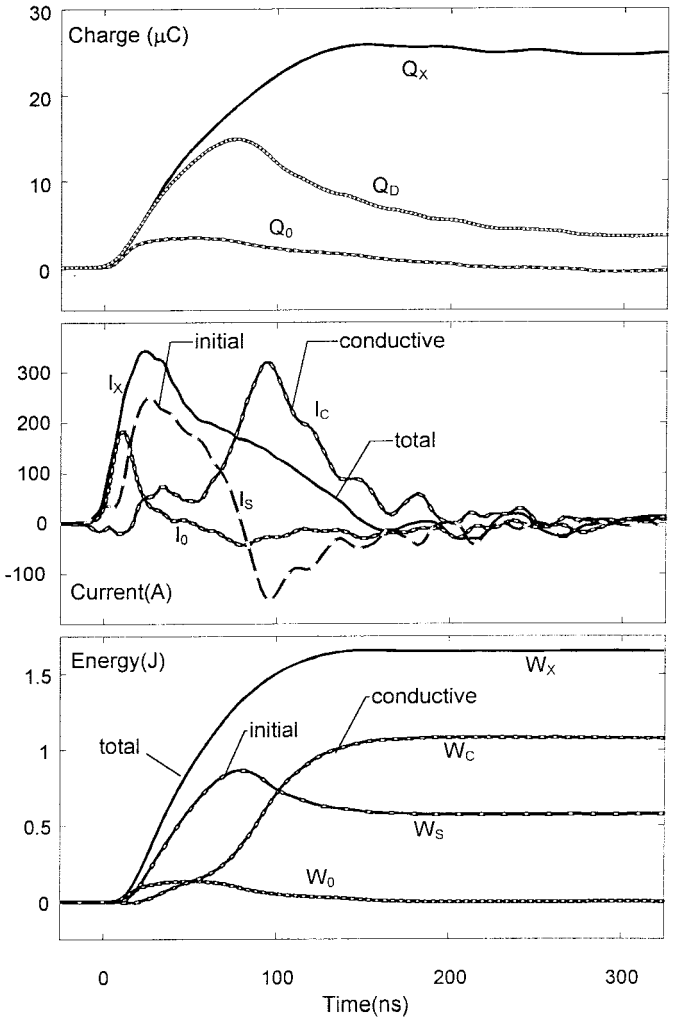

Fig. 7. Energy input during corona development. Measured current, charge, and energy input of both initial and conductive streamer phase.

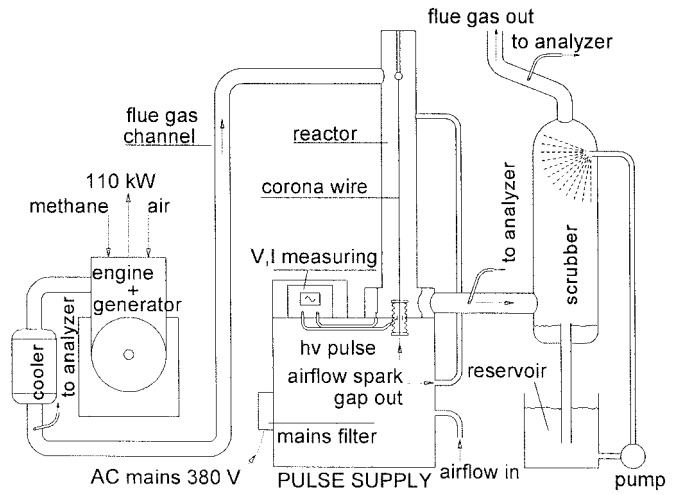

Fig. 8. The pilot unit installed in the flue gas system of a 110 kW cogeneration installation.

engine is an attractive option for CO_2 recycling applied to crops growing. Initial tests were performed at an industrial combined heat and power (CHP) site. An overview of the setup is given in Fig 8.

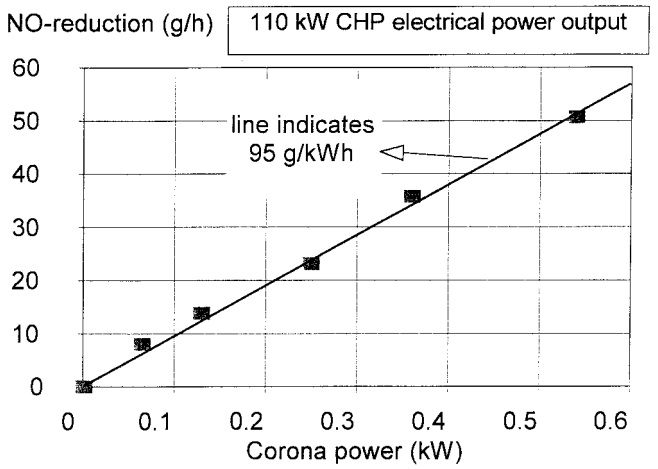

Fig. 9. Results of the flue gas tests. NO removal as a function of corona power.

During generation of 110 kW of electrical power, the flue gas was treated by the pulsed corona pilot unit. The unit was running at a corona power level of up to 600 W. NO removal (oxidation into NO_2) was determined in terms of g/h (NO and total NO_x measurements were taken before the scrubber and before the reactor, nitric acid was not measured). Removal of other flue gas fractions such as ethylene was found to be minimal, most probably due to the large NO load of 1.6 kg/h. NO has the lowest apparent activation energy and is therefore processed more easily. Fig. 9 shows the resulting NO-removal rate as a function of corona power. Since a relatively small fraction of the high NO load was removed, we see a high removal efficiency (95 g/kWh). It is clear that we are in the initial part of the exponential function $X(E)$ given in (4).

In the laboratory it was clearly shown that styrene, toluene, ethylene, and NO-ethylene mixtures can be decomposed to a high degree with our pulsed corona reactor. The VOC's propane, butane, pentane, and 1,1,1 trichloro-ethane are not completely decomposed. Table I gives an overview of chemical measurements. We now compare the calculated conversion using (4) and the measured conversion. It is found that the model fits in the cases of: styrene, toluene, 1,1,1 trichloroethane, ethylene, NO, and pentane. The conversion for propane and butane calculated with (4) does not fit the experimental data. Part of this conversion may require additional intermediate products which is not in line with the assumption of a first order reaction. Fitted values for ΔE_0 are summarized in Table I. The fit for toluene is illustrated in Fig. 10 by a graph of measured values X_{measured} (amount removed divided by amount on input both taken from toluene measurements) versus calculated values for the conversion, X_{model} (amount removed divided by amount on input as calculated from (4) by using the measured corona energy density and the fitted value for the apparent activation energy). Here the full range of residence times, concentrations, and corona energies is covered by (4) and a single value for ΔE_0.

Apparent activation energies found in this work are compared with ΔE_0 values derived from results of other researchers [16]–[22]. A summary can be found in Table II.

TABLE I
OVERVIEW OF CHEMICAL MEASUREMENTS AND DECOMPOSITION OF VOC'S IN AIR. THE VALUES FOR THE APPARENT ACTIVATION ENERGY ΔE_0 ARE FITTED ACCORDING TO (4) AND (6)

		Input Range			Measured Data	
Substance	M [kg/ kmol]	Concentration [ppm]	Mass flow [g/h]	Corona Power [kW]	Corona energy kWh per kg load to reach 63% removal	ΔE_0 [J/liter]
NO	30	213	6.5-23	0.15 - 1.10	15	16.5
Toluene	92	125 - 450	18-40	0.13 - 1.16	24	98.8
Styrene	104	30 -190	15-87	0.25 - 2.54	7	11.3
1,1,1 TCA	133	80 -1000	4-25	0.13 - 1.13	180	135
Pentane	72	80 -1000	6-73	0.14 - 1.04	88	185
Ethylene	28	150 - 2500	17-114	0.18 - 1.23	12	41.2
Propane	44	10 - 500	1.7-36	0.16 - 1.15	180	-
Butane	58	50 - 2000	9-111	0.14 - 1.19	75	

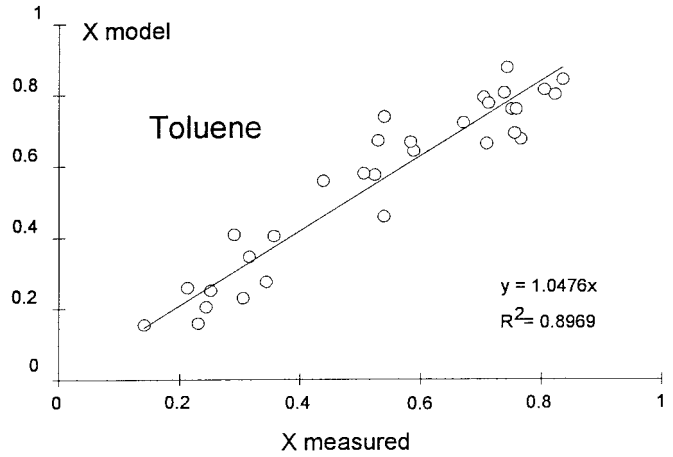

Fig. 10. Measured conversion of toluene versus calculated conversion using the model represented by (4). The full range of flow rates, input concentrations, and applied corona power is covered.

TABLE II
APPARENT ACTIVATION ENERGIES ΔE_0 [J/liter] FROM THIS WORK AND FROM THE WORK BY ROUSH ET AL. [21], COMPARED WITH DATA DERIVED FROM THE WORK OF PENETRANTE ET AL. [16]–[20] AND THE WORK OF COOGAN ET AL. [22]. REMOVAL IS $X = 1 - \exp[-E/\Delta E]$, WHERE E IS THE APPLIED CORONA ENERGY PER UNIT VOLUME

Substance	This Work pulsed corona	LANL [22] barrier discharge	LLNL [16-20] pulsed corona	LLNL [16-20] e-beam	Roush-Hutherson [21] pulsed corona
NO	16.5		50	10	10-21
Toluene	98.8	120			91-253
Styrene	11.3				
$C Cl_4$			219 *555*	44 *9*	
TCA (1,1,1)	135				
TCE		80	*16*	*9*	
Benzene			*500*	*39*	
Pentane	185				
Ethylene	41.2				
Propane	do not fit model				
Butane					

Remarks:
- LANL in N_2, 20 % O_2, 1% H_2O
- LLNL normal: in N_2
  italics: in dry air
- Roush-Hutherson values depending on pulse parameters

VII. EFFICIENCY

The transport of energy from mains AC power to chemical processes can be divided in three separate conversion steps [23].

1) Energy from mains power into high-voltage pulses.
2) High-voltage energy into corona discharge energy in the gas.
3) Corona energy finally used for chemical processes.

The NO removal process was chosen for investigation of the efficiencies of the three separate steps of energy transport. At the same time we investigated the effect of polarity on these efficiencies. An overview of the results is given in Fig. 11.

The conversion in steps 1) and 2) was determined from the electrical measurements on mains power and on corona power.

The application of corona energy for chemical processes, step 3), was expressed as amount of substance processes per kWh of the corona energy from step 2). Step 3) is found to be independent of polarity, i.e., chemistry is polarity independent here.

Step 2) energy transfer, however, is very much affected by polarity choice. A positive wire gives a better energy transfer when polarity effects are compared at the same external voltage. As we know from previous work [1], a negative wire

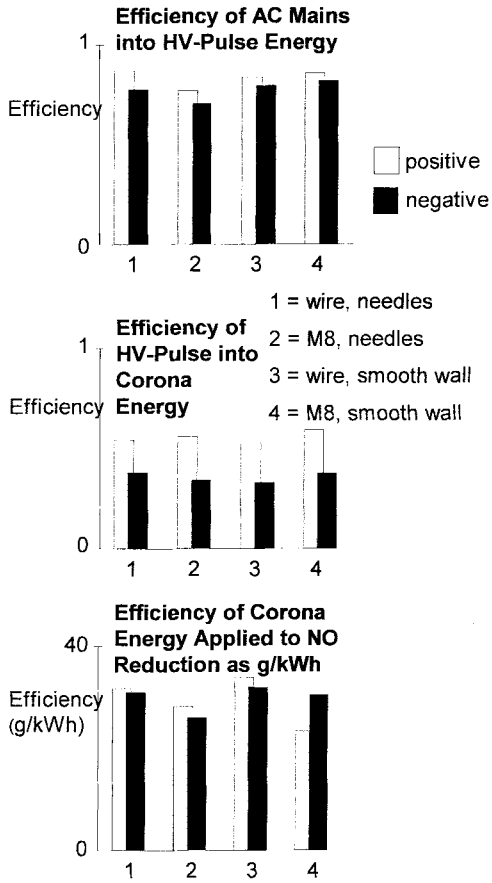

Fig. 11. Effect of polarity on energy conversion and chemical processing of NO in the pilot reactor.

needs a higher voltage to produce intense coronas. This effect is not accounted for in this study, we applied the same voltage level for both polarities.

VIII. Conclusions

Simultaneous recordings with CCD camera and electrical diagnostics allow a clear analysis of the high intensity corona development. Initial streamer phase and transition to a conductive streamer phase are detected and an excellent correlation is found between all data from electrical records and CCD movies. The energy input during the various streamer developments was followed.

Chemical conversion processes initiated by the pulsed corona were tested in the lab but also at industrial locations. A model that only needs two parameters, apparent activation energy and corona energy, can in many cases explain the VOC's removal. Many experiments fit the model. Butane and propane do not fit probably due to a departure from the assumption we made on the reaction type.

With respect to pulsed power, reliability can be further increased from the established 350 h of continuous operation to considerably longer times.

The EMC of pulsed power for pollution control can be designed to perform perfectly. Following a well-defined approach, pulsed power was constructed such that no interference at all occurred with surrounding and internal equipment.

Acknowledgment

The authors would like to thank the many members of the staff and students from the high-voltage and separations technology groups for their valuable contributions.

References

[1] P. P. M. Blom, "High power pulsed corona," Ph.D. dissertation, Eindhoven University of Technology, The Netheralnds, Feb. 1997.
[2] B. M. Penetrante and S. E. Schultheis, Eds., "Nonthermal plasma techniques for pollution control, Part B: Electron beam and electrical discharge processing," in *NATO ASI Series*. Berlin, Germany: Springer-Verlag, 1993.
[3] A. P. Gelbein, Ed., "Managing hazardous waste with electricity," *Chemtech, Amer. Chem. Soc.*, vol. 26, no. 4, Apr. 1996.
[4] E. J. M. van Heesch, A. J. M. Pemen, and P. C. T. van der Laan, "Pulsed corona existence up to 850°C," in *Proc. 6th Int. Symp. High-Voltage Eng.*, New Orleans, LA, 1989, p. 4.
[5] S. A. Vitale, L. Bromberg, K. Hadini, P. Falkos, and D. R. Kohn, "Decomposing VOC's with an electron beam plasma reactor," *Chemtech, Amer. Chem. Soc.*, vol. 26, no. 4, pp. 58–63, Apr. 1996.
[6] M. A. van Houten, "Electromagnetic compatibility in high-voltage engineering," Ph.D. dissertation, Eindhoven University of Technology, The Netherlands, Oct. 1990.
[7] P. C. T. van der Laan and A. P. J. van Deursen, "Linear EMC-methods applied to power systems," in *Proc. 10th Int. Symp. High-Voltage Eng.*, Montreal, Canada, Aug. 25–29, 1997, vol. 1, pp. 59–66,.
[8] I. A. D. Lewis and F. H. Wells, *Millimicrosecond Pulse Techniques*, 2nd ed. London: Pergamon, 1959, pp. 109–111.
[9] G. G. Wolzak, "The development of high-voltage measuring techniques," Ph.D. dissertation, Eindhoven University of Technology, The Netherlands, Dec. 1983.
[10] S. Shihab, "A fast response impulse voltage measuring system for testing of gas insulated substations equipment," *IEEE Trans. Power Delivery*, vol. PWRD-1, no. 3, pp. 42–47, 1986.
[11] E. J. M. van Heesch, P. P. M. Blom, and P. C. T. van der Laan, "An E field and ion sensor for high intensity pulsed coronas," in *21st Int. Conf. Phenomena Ionized Gases*, Bochum, Germany, Sept. 19–24, 1993, pp. 329–330.
[12] O. J. Tassicker, "Measurement of corona current density at an electrode boundary," *Electron. Lett.*, vol. 5, no. 13, pp. 285–286, 1996.
[13] R. T. Waters, "Diagnostic techniques for discharges and plasmas," in *Electrical Breakdown and Discharges in Gases, NATO ASI Series.* New York: Plenum, 1983, vol. B, no. 89b, pp. 203–265.
[14] S. V. B. van Paasen, H. W. M. Smulders, A. J. P. M. Staring, K. J. Ptasinski, F. M. van Gompel, and E. J. M. van Heesch, "Decomposition of VOC's in a continuous high-voltage pulsed corona process," *Proc. 10th Int. Symp. High-Voltage Eng.*, Montreal, Canada, 1997, vol. 6, pp. 365–368.
[15] L. A. Rosocha, G. K. Anderson, L. A. Bechtold, J. J. Coogan, H. G. Heck, M. Kang, W. H. McCulla, R. A. Tennant, and P. J. Wantuck, "Treatment of hazardous organic wastes using silent discharge plasmas," *Nonthermal Plasma Techniques for Pollution Control, Part B.* Berlin, Germany: Springer-Verlag, 1993, pp. 281–308.
[16] B. M. Penetrante, M. C. Hsiao, B. T. Merritt, G. E. Vogtlin, and P. H. Wallman, "Comparison of electrical discharge techniques for nonthermal processing of NO in N_2," *IEEE Trans. Plasma Sci.*, vol. 23, no. 4, pp. 679–687, 1995.
[17] B. M. Penetrante, M. C. Hsiao, B. T. Merritt, G. E. Vogtlin, and P. H. Wallman, "Electron-impact dissociation of molecular nitrogen in atmospheric-pressure nonthermal plasma reactors," *Appl. Phys. Lett.*, vol. 67, no. 21, pp. 3096–3098, 1995.
[18] B. M. Penetrante, M. C. Hsiao, J. N. Bardsley, B. T. Merritt, G. E. Vogtlin, P. H. Wallman, A. Kuthi, C. P. Burkhart, J. R. Bayless, "Electron beam and pulsed corona processing of carbon tetrachloride in atmospheric pressure gas streams," *Phys. Lett. A*, vol. 209, pp. 69–77, 1995.
[19] B. M. Penetrante, M. C. Hsiao, B. T. Merritt, G. E. Vogtlin, and P. H. Wallman, "Pulsed corona and dielectric barrier discharge processing of NO in N_2," *Appl. Phys. Lett.*, vol. 68, no. 26, pp. 3719–3721, 1996.
[20] B. M. Penetrante, M. C. Hsiao, B. T. Merritt, G. E. Vogtlin, and P. H. Wallman, "Electron beam and pulsed corona processing of volatile organic compounds in gas streams," *Pure and Appl. Chem.*, vol. 68, no. 5, pp. 1083–1087, 1996.
[21] R. A. Roush, R. K. Hutcherson, M. W. Ingram, and M. G. Grothaus, "Effects of pulse risetime and pulse width on the destruction of toluene

and NO_x in a coaxial pulsed corona reactor," in *Conf. Record 22nd Int. Power Modulator Symp., IEEE*, Boca Raton, FL, 1996, pp. 79–84.

[22] J. J. Coogan, L. A. Rosocha, M. Garcia, H. Garcia, R. A. Korzekwa, H. E. Canavan, and Z. Falkenstein, "Barrier discharge treatment of VOC's in oxygen lean mixtures," presented at the *AOTs-2 Conf.*, London, Canada, Sept. 1995.

[23] H. W. M. Smulders, F. M. van Gompel, S. V. B. van Paasen, E. J. M. van Heesch, and P. C. T. van der Laan, "Efficiency and reliability of a repetitive pulse source for continuous pulsed corona processes," in *Proc. 10th Int. Symp. High-Voltage Eng.*, Montreal, Canada, Aug. 25–29, 1997, vol. 6, pp. 393–396.

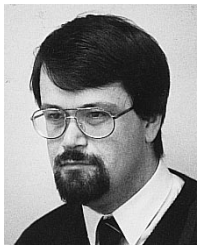

Erwin H. W. M. Smulders was born in Tilburg, The Netherlands, in August 1960. He received the M.Sc. degree in electrical engineering in 1994 from the Eindhoven University of Technology, The Netherlands.

Since 1995, he has been employed on the Pulsed Corona Pilot Project of the High-Voltage and EMC group of the EUT. His interests are high-voltage techniques, EMC, pulsed power, and the influence of electrical energy on chemical processes.

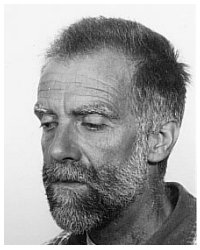

Bert E. J. M. van Heesch was born in 1951 in Utrecht, The Netherlands. He received the master's degree in physics in 1975 and the Ph.D. degree in plasma physics and fusion related research in 1982.

He has been leading Eindhoven corona and pulsed power research since 1986. Prior, he was occupied with fusion technology in Jutphaas, The Netherlands, in Suchumi, Russia, and Saskatoon, Canada. Among his designs are a toroidal fusion experiment (5 GW pulse power), a particle beam diagnostic, a substation high-voltage measuring system, and a unit for continuous pulsed power corona.

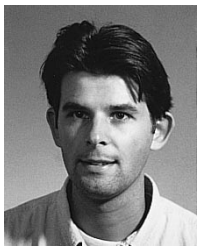

Sander S. V. B. van Paasen was born in Ysselstein, The Netherlands, in 1972. He received the degree in chemical engineering from the Eindhoven Polytech, The Netherlands, in 1993, and the M.Sc. degree in chemical engineering from Eindhoven University of Technology in 1996.

After his degree he joined the Process Technology Group and High-Voltage and EMC Group at the Eindhoven University to participate in the pulsed corona project for gas treatment. Since 1997 he has worked as a process and product designer in trainee-ship at the University.